

XXXVII IBERIAN LATIN AMERICAN CONGRESS  
ON COMPUTATIONAL METHODS IN ENGINEERING  
BRASÍLIA - DF - BRAZIL

## NONLINEAR DYNAMICS OF A VIBRATION-BASED ENERGY HARVESTING SYSTEM USING PIEZOELECTRIC AND SHAPE MEMORY ALLOY ELEMENTS

### **Arthur Adeodato**

adeodatoarthur@hotmail.com

CEFET/RJ, Department of Mechanical Engineering 20.271.110, Rio de Janeiro - RJ – Brazil

### **Luciana Loureiro da Silva Monteiro**

lucianals@lts.coppe.ufrj.br

CEFET/RJ, Department of Mechanical Engineering 20.271.110, Rio de Janeiro - RJ – Brazil

### **Paulo Cesar da Camara Monteiro Junior**

camara@lts.coppe.ufrj.br

Universidade Federal do Rio de Janeiro, COPPE – Department of Ocean Engineering, RJ – Brazil

### **Flavio Maggessi Viola**

fmviola@gmail.com

CEFET/RJ, Department of Mechanical Engineering 20.271.110, Rio de Janeiro - RJ – Brazil

### **Sergio Almeida Oliveira**

amserol@yahoo.com.br

CEFET/RJ, Department of Mechanical Engineering 20.271.110, Rio de Janeiro - RJ – Brazil

### **Pedro Manuel Calas Lopes Pacheco**

pmcl.pacheco@gmail.com

CEFET/RJ, Department of Mechanical Engineering 20.271.110, Rio de Janeiro - RJ – Brazil

### **Marcelo Amorim Savi**

savi@mecanica.coppe.ufrj.br

Universidade Federal do Rio de Janeiro, COPPE – Department of Mechanical Engineering, MECANON, RJ – Brazil

**Abstract.** *Energy harvesting is the conversion of available mechanical vibration energy into electrical energy that can be employed for different purposes. Several works have investigated the development of linear vibration energy harvesters that are efficient in a very narrow bandwidth around the fundamental resonance frequency. Nowadays, many researches have included different kinds of nonlinearities to expand the bandwidth of the energy harvesters. This paper deals with the use of smart materials for energy harvesting purposes. Basically, piezoelectric and shape memory elements are combined to build an energy harvesting system. The analysis is developed considering a one-degree of freedom mechanical system where the equation of motion is formulated by assuming the electro-mechanical coupling provided by a piezoelectric element and the restitution force provided by shape memory element described using a polynomial constitutive model. Numerical results indicate that the inclusion of the SMA element can dramatically change system dynamics, showing different kinds of responses including periodic and chaotic regimes.*

**Keywords:** *Piezoelectric material, Shape memory alloy, Energy harvesting, Nonlinear dynamics*

## 1 INTRODUCTION

The development of wireless sensor networks is the subject of several studies. In recent years, the purpose of powering these devices using vibration-based energy harvesting have received a lot of attention due to their growing importance since it can be used in many applications in case of inaccessible or hostile environments. Several methods have been used to convert environmental mechanical energy into electric energy, such as electrostatic (Round et al. 2013), electromagnetic (Mitcheson et al. 2004), and piezoelectric methods (Yang et al. 2009).

Piezoelectric material has the ability to convert mechanical strain into electrical charge and also have the opposite effect, the application of electric voltage produces mechanical strain. In this regard, piezoelectric materials can be used as transducers and sensors used in different kinds of applications (Erturk and Inman 2011a).

Solutions for vibration-based energy harvesting system using piezoelectric materials have been mostly studied in recent years. They are usually employed for electro-mechanical conversion due to high output power density and energy conversion efficiency (Anton & Sodano 2007); (Erturk and Inman 2011a,b); (Dutoit and Wardle 2006).

Usually, linear energy harvesting systems exploit excitations close to the resonant conditions. Therefore, if the excitation vibration frequency deviates slightly from this resonance condition, the electrical power output is drastically reduced (Beeby et al., 2013). Since vibration systems are usually related to signals with different frequencies and amplitudes, various strategies have been used to increase the frequency range of operation of energy harvester. In this regard, mechanical nonlinearities are usually investigated in order to enhance the energy harvesting system capacity. One possibility is the inclusion of external forces to change the equivalent stiffness of the energy harvesting system and therefore its resonant frequency. The addition of external magnets to a piezoelectric cantilever beam is a possible way to introduce nonlinearities on mechanical systems (Erturk and Inman, 2009; Staton et al., 2010). Ferrari et al. (2010) have developed a piezoelectric beam converter coupled to permanent magnets to create a bistable system. Under proper conditions, the nonlinear system has a wider bandwidth than the linear configuration. Stanton et al. (2010)

analyzed a nonlinear energy harvester capable of bidirectional hysteresis using a piezoelectric beam with a permanent magnet end mass. Either the softening or the hardening responses were obtained, allowing frequency response to be extended bidirectionally using an experimental approach. De Paula et al. (2015) investigated random aspects on vibration-based energy harvesting of a piezomagnetoelastic structure. A comparison between linear, nonlinear bistable and nonlinear monostable mechanical systems subjected to random excitations showed an enhancement of harvested power in a bistable system. Cammarano et al. (2014) exploited a comparison between the bandwidths of linear and nonlinear energy harvesters showing that the complex dependence of the response upon the input excitation makes the comparison of linear harvesters with nonlinear energy harvesters challenging, showing the importance of studies concerning nonlinear effects of energy harvesting.

The synergistic use of smart materials is a new challenge related that can be exploited for energy harvesting purposes. The inclusion of shape memory alloys (SMAs) elements can enhance energy harvesting performance. SMAs present martensitic phase transformation that can be exploited either to change stiffness or to dissipated energy. Savi and Pacheco (2002) showed the nonlinear dynamics of shape memory systems considering single and two-degree of freedom oscillators coupled shape memory oscillators. Results indicated nonlinear characteristics such as dynamic jumps and chaos. Silva et al. (2015) employed a numerical analysis of a SMA-piezoelectric energy harvesting systems where the thermomechanical of SMA is described by Brinson's model. Results indicated that the inclusion of the SMA element can be used to extend the operational range of the system. Rhimi and Lajnef (2012) studied the power, frequency and time response of a cantilevered composite beam containing piezoelectric ceramic and shape memory alloy cylindrical inclusions, showing the nonlinear behavior due to the phase transformation within the SMA inclusions. Avirovik et al. (2013) developed a hybrid device coupling piezoelectric element with SMA for dual functionality, both as an actuator and an energy harvester.

This paper deals with the synergistic use of SMA and piezoelectric elements on vibration-based energy harvesting systems. The analysis is developed considering a one-degree of freedom mechanical system where the equation of motion is formulated by assuming a polynomial constitutive model (Falk, 1980) to describe the thermomechanical behavior of the SMA element. Numerical results indicate that the inclusion of the SMA element can dramatically change system dynamics, showing different kinds of responses including periodic and chaotic regimes. Despite the simplicity of the polynomial model used to capture shape memory and pseudoelastic effects, its nonlinear dynamic response may represent the qualitative response of combined piezoelectric and shape memory alloy energy harvester system.

## 2 PIEZOELECTRIC CONSTITUTIVE MODEL

This section is devoted to the one-dimensional constitutive equations of linear piezoelectric material that presents electromechanical coupling being possible as direct and inverse operation modes. The inverse effect is associated with the generation of strain/stress in response to an applied electrical field; on the other hand, the direct effect is related to electrical charge that is a response to an applied strain/stress.

A usual configuration of an energy harvesting system is based on a cantilever beam, where the generator beam may have one or two piezoelectric layers attached to a substrate rigidly clamped at one end. The PZT beam operating in a bending mode is subjected either to tensile or compressive stresses and produces electrical voltage. Figure 1 shows a piezoelectric behavior of a thin structure is such that it can be modeled as a beam that shear stress are negligible and the main stress only depends on the one-dimensional bending normal stress (Erturk and Inman 2011a)

$$\varepsilon = s^E \sigma + dE \quad (\text{inverse effect}) \quad (1)$$

$$D = d\sigma + \epsilon^\sigma E \quad (\text{direct effect}) \quad (2)$$

where  $a$ ,  $b$  and  $h$  are the length, the width and the thickness of the beam,  $\varepsilon$  is the strain,  $\sigma$  is the stress,  $D$  is the electric displacement, and  $E$  is the electric field. The piezoelectric coefficient, elastic compliance and permittivity are denoted respectively by  $d$ ,  $s$  and  $\epsilon$ . The superscripts  $E$  and  $\sigma$  denote that the respective constants are evaluated at constant electric field and stress, respectively.

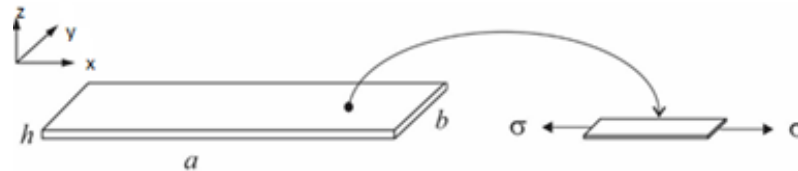


**Figure 1. Thin piezoelectric beam.**

### 3 SHAPE MEMORY ALLOY CONSTITUTIVE MODEL

The one-dimensional polynomial model proposed by Falk (1980) is used to describe the restitution force provided by shape memory alloy in energy harvester system. In this model, the only state variables are strain  $\varepsilon$  and temperature  $T$ . It is defined a free energy density considering a polynomial form that depends on strain and temperature. The minimum or maximum points represent stability and instability of each SMA macroscopic phase. Basically, it is considered austenite ( $A$ ) and two variants of martensite,  $M+$  induced by tension and  $M-$  induced by compression. Based on this, the free energy potential is defined as follows,

$$W(\varepsilon, T) = \frac{c}{2}(T - T_M)\varepsilon^2 - \frac{d}{4}\varepsilon^4 + \frac{d^2}{24c(T_A - T_M)}\varepsilon^6 \quad (3)$$

where  $c$  and  $d$  are material constants, and  $T_A$  is the temperature above which austenite is stable and  $T_M$  is the temperature below which martensite is stable. Thus, the stress equation is given by the derivative of the free energy with respect to strain:

$$\sigma = c(T - T_M)\varepsilon - d\varepsilon^3 + \frac{d^2}{4c(T_A - T_M)}\varepsilon^5 \quad (4)$$

Figure 2 shows free energy versus strain curves for three different temperatures using the  $c = 1 \times 10^3$  MPa/K,  $d = 40 \times 10^6$  MPa/K;  $T_M = 287$ K;  $T_A = 313$ K (Paiva and Savi, 2006). When  $T > T_A$  the system has only one fixed point (equilibrium of the austenitic phase),  $T_A > T > T_M$  the system has three minima corresponding to three stable phases-austenite (A), and detwinned martensite induced by tension ( $M+$ ) and by compression ( $M-$ ) and  $T < T_M$  the system has two minima at nonvanishing strains, where martensite is stable. Figure 3 shows the corresponding stress versus strain curves.

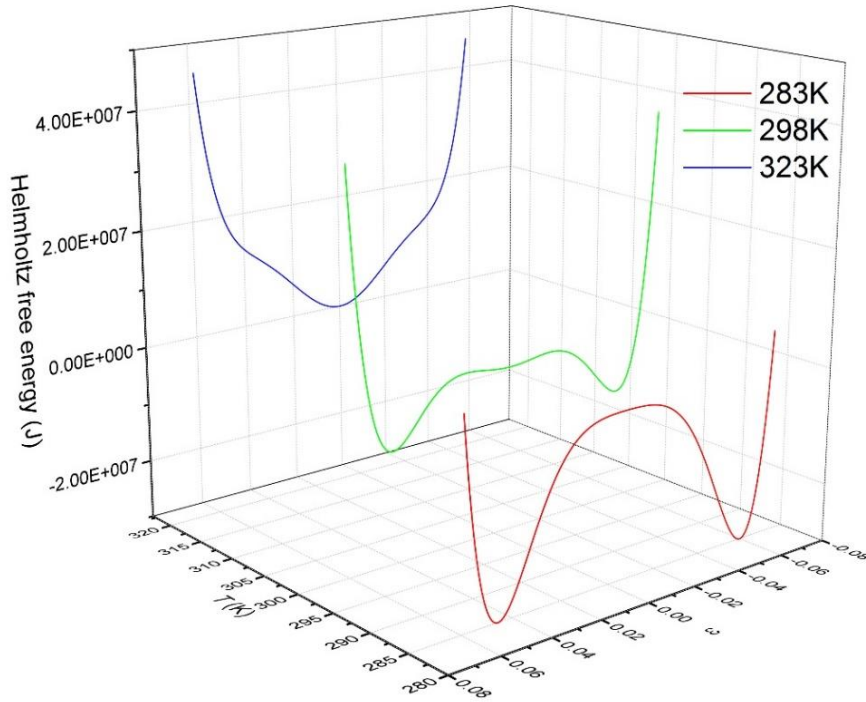


**Figure 2: Free energy versus strain for different temperatures.**

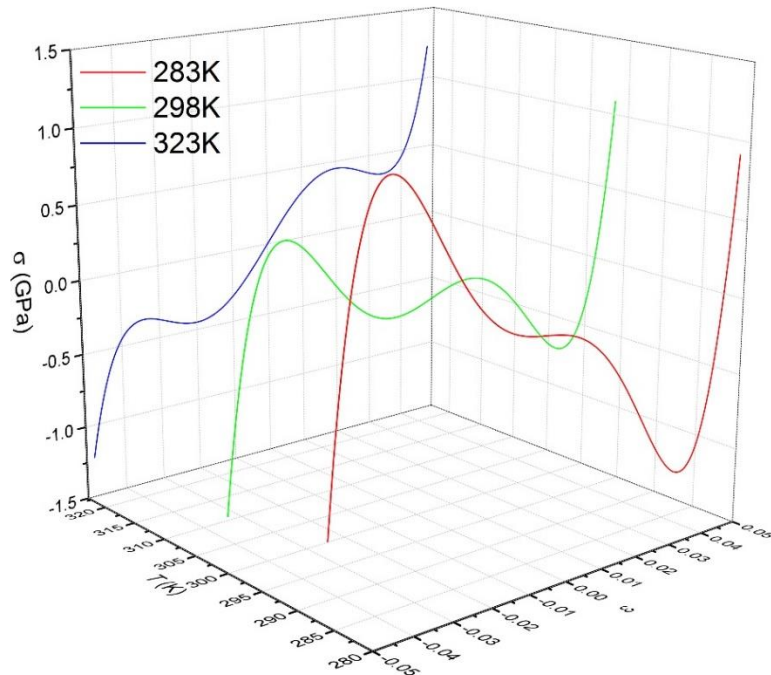


**Figure 3: Stress versus strain for different temperatures.**

#### 4 VIBRATION-BASED ENERGY HARVESTING

In order to perform the dynamical analysis of energy harvesting system with SMA element, a single degree of freedom oscillator can be seen in Fig. 4. The lumped-parameter modelling approach describes the dynamics of the point of interest, that can be the free end of piezoelectric beam (Figure 1) using lumped parameters, which are the equivalent mass, stiffness, damping, electro-mechanical coupling. In this model,  $m$  represents the mass, the displacement is  $y$ ; the base excitation is represented by  $u=u(t)$  while  $z$  represents the mass displacement relative to the base. In addition, the oscillator has a linear viscous damping with coefficient  $b$ . The SMA element may be considered as a bar with length  $l$  and cross-sectional area  $A$ , presenting a restitution force given by  $\sigma A$ , where  $\sigma$  is described by the constitutive equations presented in the previous section. Electro-mechanical coupling is provided by a piezoelectric element with coupling coefficient  $\hat{\chi}$ . This element is connected to an electric circuit represented by an electrical resistance  $R$  and capacitance  $C_p$ ;  $V$  is the voltage across the piezoelectric element.



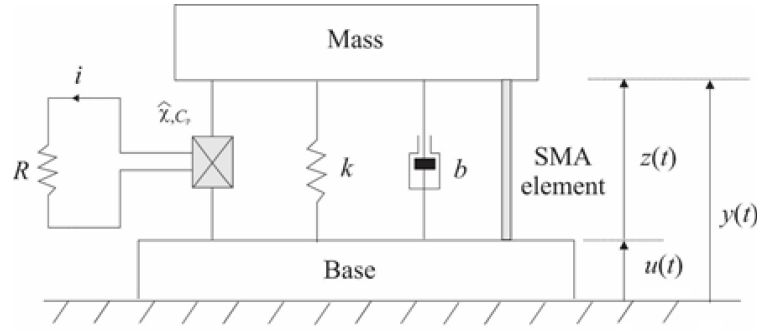


**Figure 4. Archetypal model of the vibration-based energy harvesting system**

The energy harvesting system could be described using the coupled equations (mechanical and electrical) are described by:

$$m\ddot{z} + b\dot{z} + kz - \hat{\chi}V + \left[ c(T - T_M)z - dz^3 + \frac{d^2}{4c(T_A - T_M)}z^5 \right] A = -m\ddot{u} \quad (5)$$

$$\hat{\chi}\dot{z} + C_p\dot{V} + \frac{1}{R}V = 0 \quad (6)$$

A dimensionless analysis of piezoelectric vibration energy harvester mathematical model is now in focus. Hence, consider spatial and electrical new coordinates as  $x = z/l$ ,  $v = V/\hat{V}$  and  $\theta = T/T_M$  where  $l$  is a reference length and  $\hat{V}$  is a reference voltage. It is defined a reference frequency  $\omega_0 = \sqrt{k/m}$  and a harmonic excitation  $-m\ddot{u} = W\cos(\omega t)$  is assumed. Using  $2\zeta = b/m\omega_0$ ,  $\chi = (\hat{V}/m\omega_0^2 l)\hat{\chi}$ ,  $\bar{c} = (AT_M/m\omega_0^2)c$ ,  $\bar{d} = (Al^2T_M/m\omega_0^2)d$ ,  $\bar{e} = Al^4d^2/[4cm\omega_0^2(T_A - T_M)]$ ,  $\lambda = 1/RC_p\omega_0$ ,  $\kappa = l\hat{\chi}/C_p\hat{V}$ ,  $\bar{\omega} = \omega/\omega_0$ , and  $\gamma = -\frac{A}{m\omega_0^2 l}$ , the equations of motion can be rewritten as follows:

$$x'' + 2\zeta x' + x - \chi v + \bar{c}(\theta - 1)x + \bar{d}x^3 + \bar{e}x^5 = \delta\cos(\bar{\omega}\tau) \quad (7)$$

$$v' + \lambda v + \kappa x = 0 \quad (8)$$

where  $(\blacksquare)' \equiv d(\blacksquare)/d\tau$ , with  $\tau$  being the non-dimensional time.

Numerical simulations are performed by employing a fourth-order Runge-Kutta method. The instantaneous non-dimensional electrical power can be obtained using the equation  $P = \lambda(v)^2$ . The following parameters are adopted for all simulations:  $\zeta = 0.01$ ,  $\chi = 0.05$ ,  $\lambda = 0.05$ ,  $\kappa = 0.5$ ,  $\bar{c} = 1.0$ ,  $\bar{d} = 1.3 \times 10^3$ ,  $\bar{e} = 4.7 \times 10^5$ , according to De Paula et al. (2015) and Savi & Pacheco (2002). The non-dimensional temperatures used for martensitic and austenitic phases are  $\theta_M = 1.0$  and  $\theta_A = 1.9$ , respectively, see Savi & Pacheco (2002).

## 5 NUMERICAL RESULTS

Numerical simulations of the energy harvesting system are treated in this section. Basically, three different aspects are of concern treating the influence of temperature, forcing frequency and forcing amplitude.

### 5.1 Influence of Temperature

The influence of the temperature is now investigated. Basically, it is considered the system response under a constant forcing frequency  $\bar{\omega} = 1.0$  and forcing amplitude  $\gamma = 0.08$ . Figure 5 presents bifurcation diagram considering induced dimensionless displacement. Figure 6 shows phase spaces and Poincaré sections for specific values of temperature. Below  $\theta_M$ , small increments in frequency can change dramatically the response, leading the system from periodic to chaotic response and vice-versa. Chaotic regions are observed in regions associated with cloud of points. Figure 7 shows the time history for two different values of the parameter  $\theta$  showing a period-1 response (a) and by increasing the temperature (b), system presents a chaotic response. Figure 8 shows the power harvested. Figure 9 shows phase spaces (power-displacement curves) and Poincaré sections for specific values of temperature.

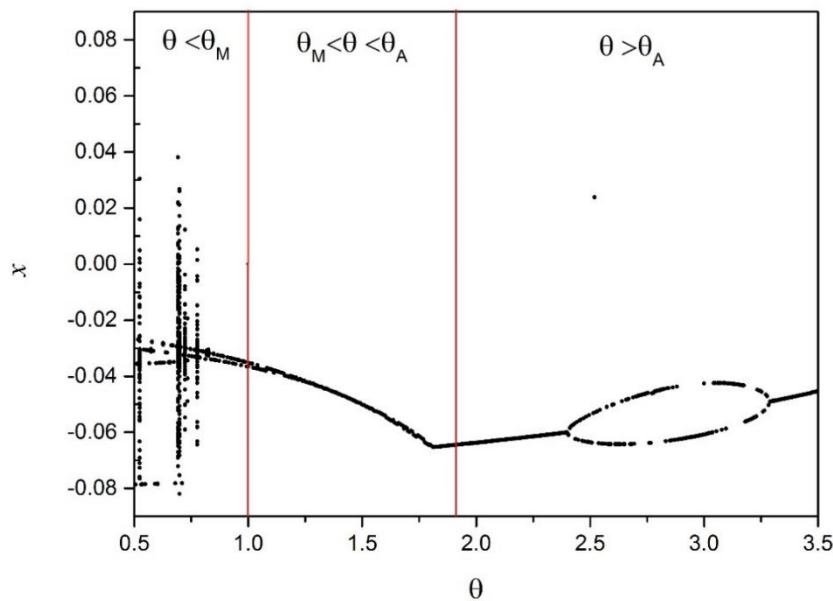
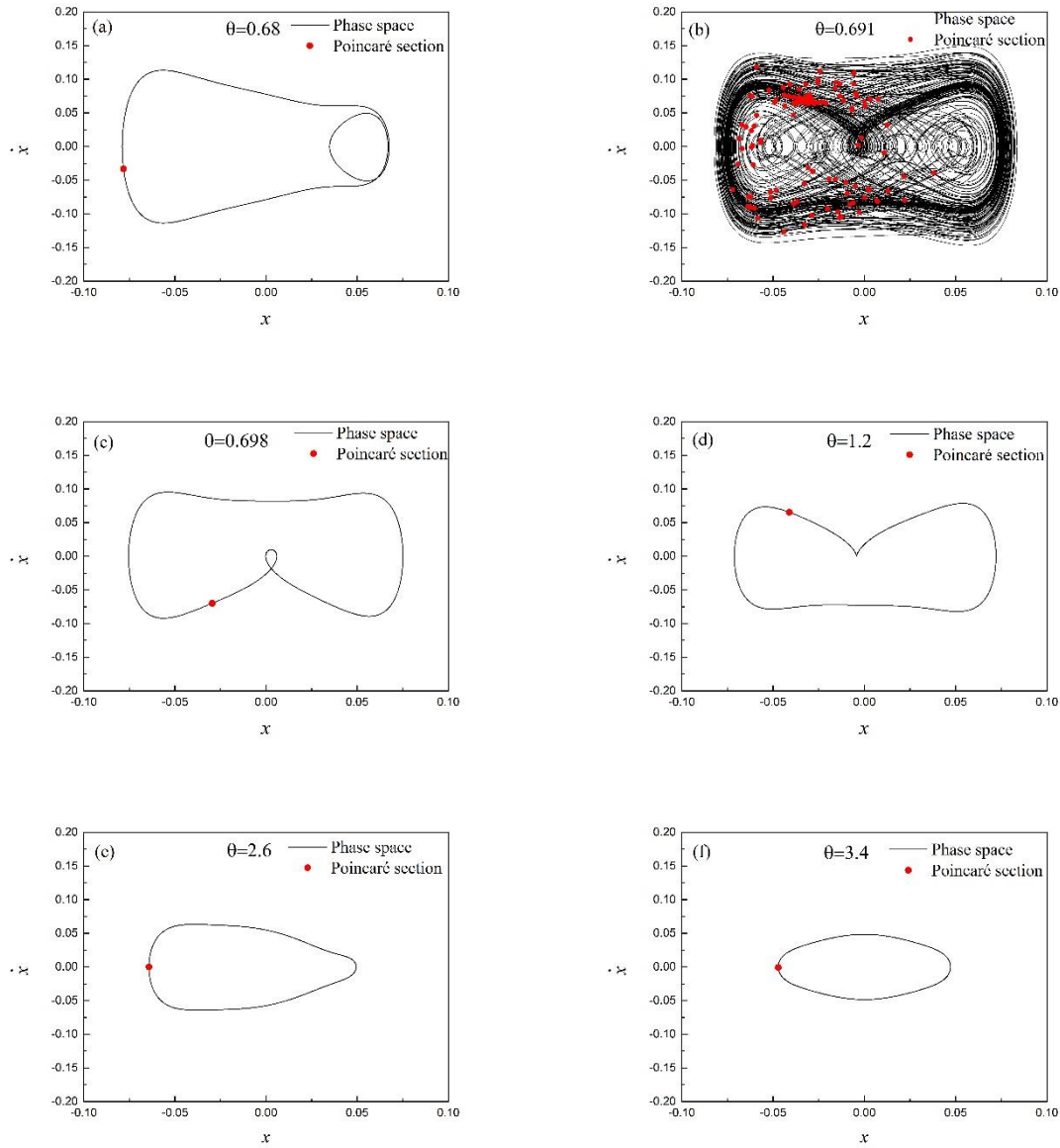


Figure 5: Dimensionless displacement considering different values of temperature.





**Figure 6: Phase space and Poincaré section for different values of temperature.**

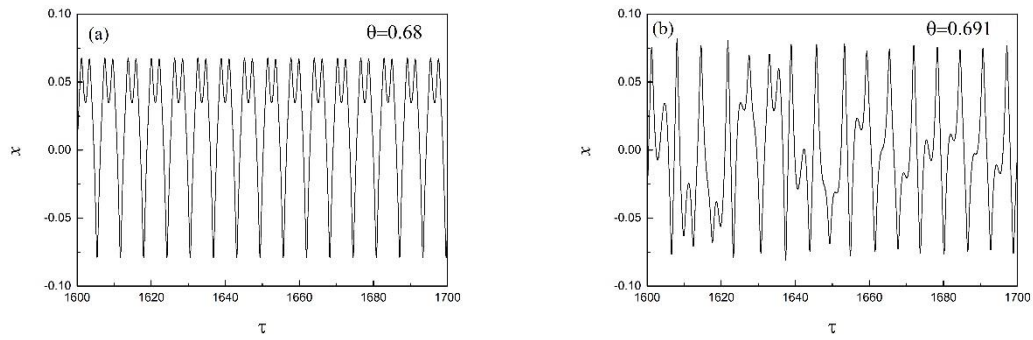


Figure 7: Time history for  $\theta=0.68$  and  $\theta=0.691$ .

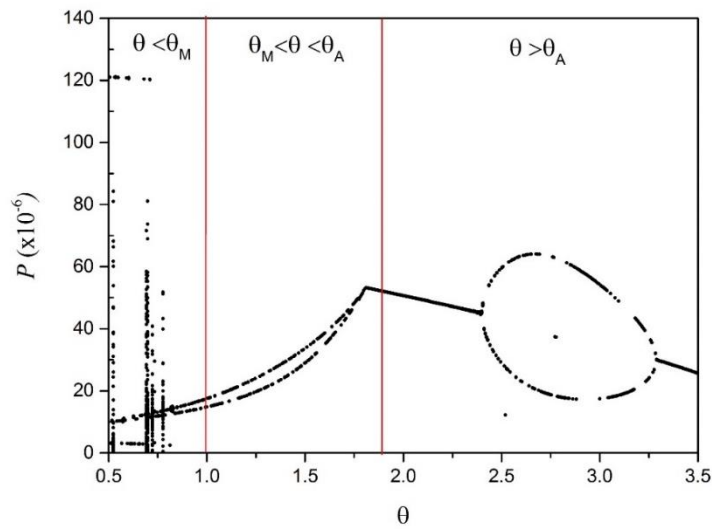
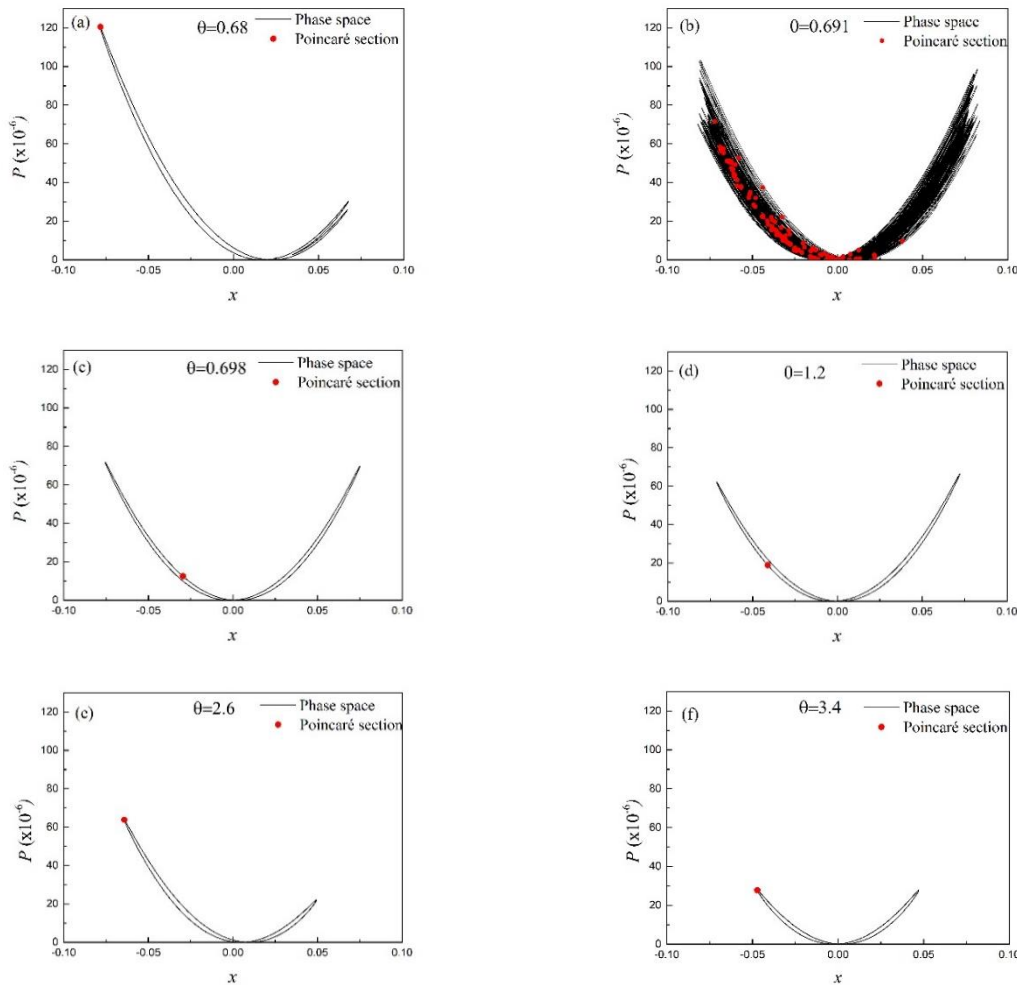


Figure 8: Power considering different values of temperature.



**Figure 9: Phase space and Poincaré section for different values of temperature.**

## 5.2 Influence of Forcing Frequency

The influence of forcing frequency at low ( $\theta < \theta_M$ ) and high ( $\theta > \theta_A$ ) temperatures is now analyzed. The forcing amplitude is assumed to be  $\gamma = 0.08$ . Figure 10 and Figure 11 present the bifurcation diagrams related to displacement and power for  $\theta = 0.7$ , respectively. For each diagram, it is identified phase space and Poincaré section for specific frequency values:  $\bar{\omega} = 0.56, 1.0$  and  $1.4$ . Different kinds of responses are observed, including periodic and chaotic responses.

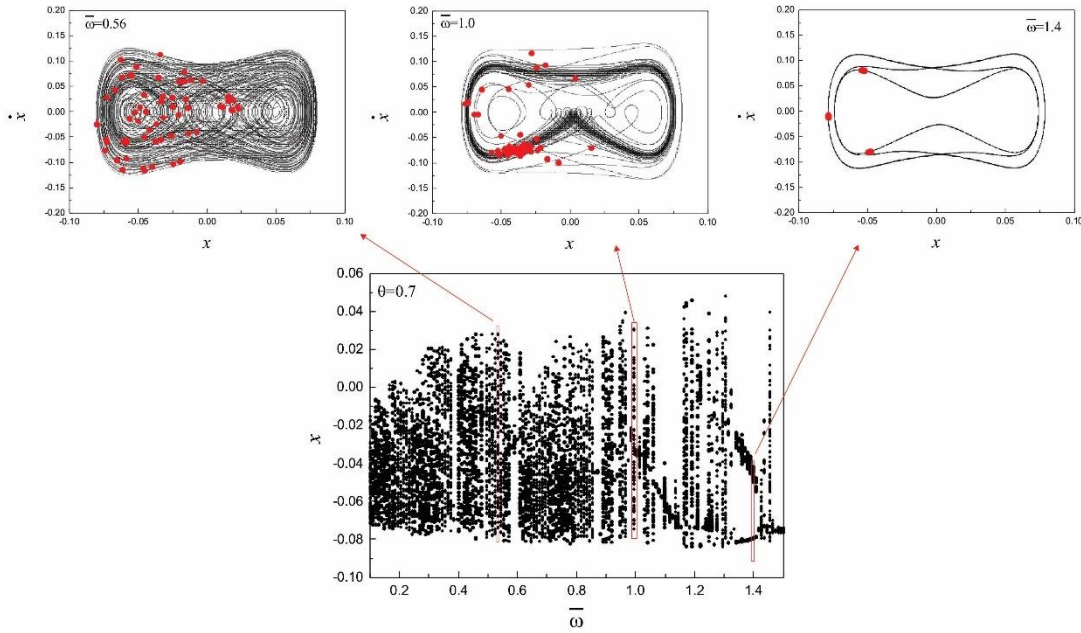


**Figure 10: Dimensionless displacement considering different values of temperature ( $\theta < \theta_M$ ).**

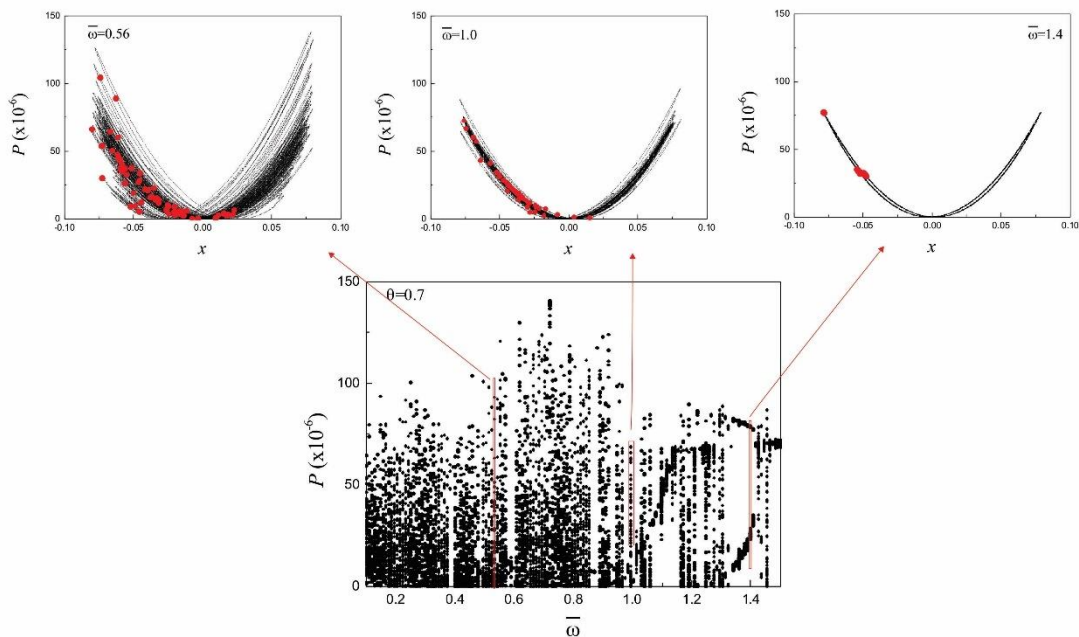


**Figure 11: Power considering different values of temperature ( $\theta < \theta_M$ ).**

Bifurcation diagrams for high temperature  $\theta = 3.5$  is now in focus. Results are presented in Figure 12 and Figure 13. By establishing a comparison with Fig. 10 and 12, it is possible to

notice that, at higher temperature, where austenitic phase is stable, the maximum values of displacement and power are smaller than at low temperature. This effect is due to SMA element stiffness that tends to be higher as temperature increases. In addition, it is observed that the system does not present chaotic response.

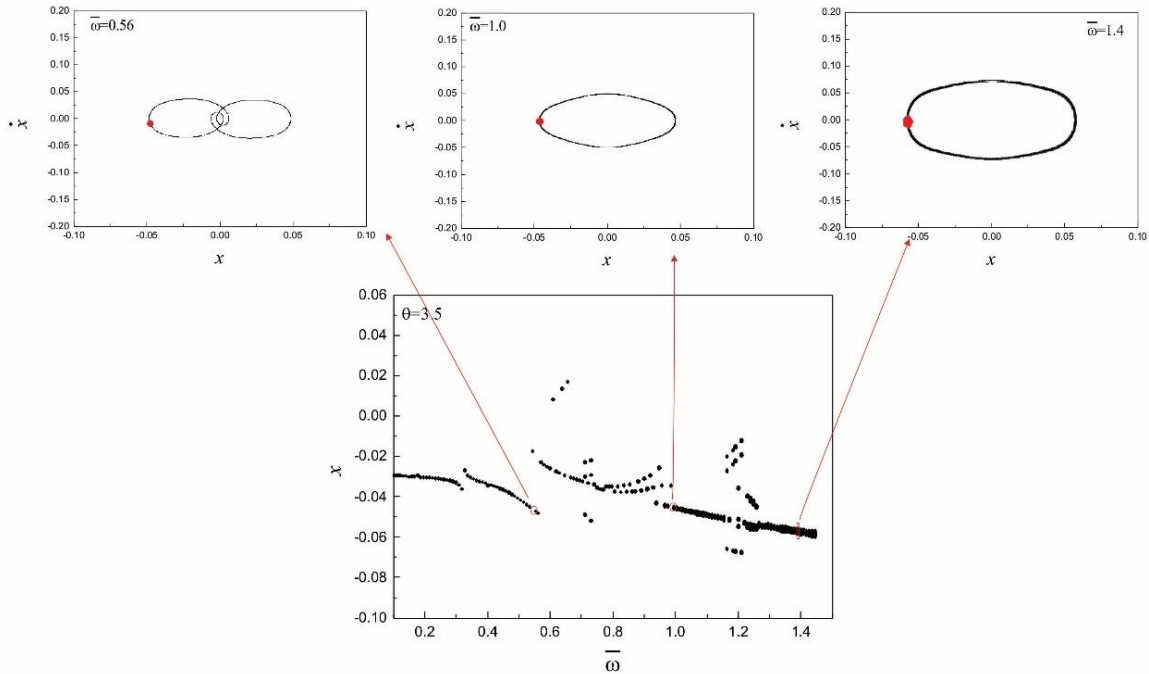


Figure 12: Dimensionless displacement considering different values of forcing frequency

$$(\theta > \theta_A).$$

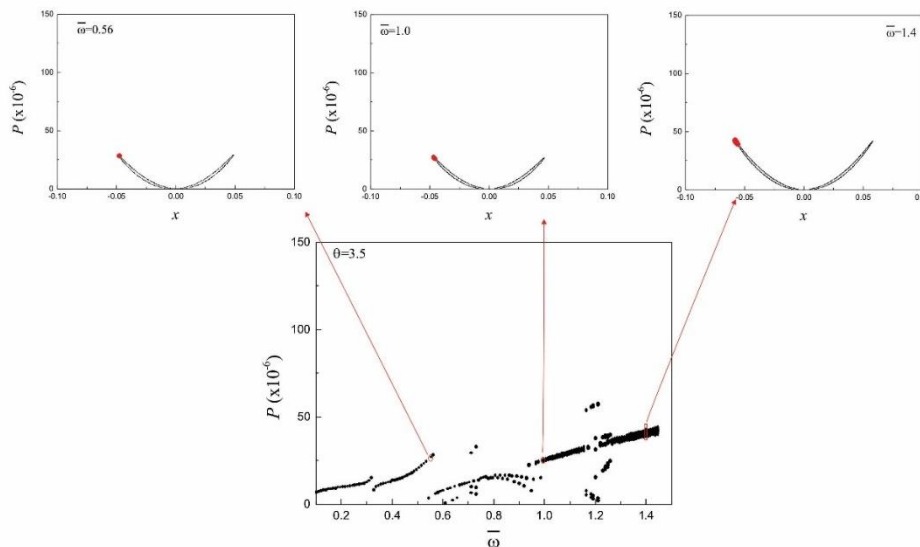
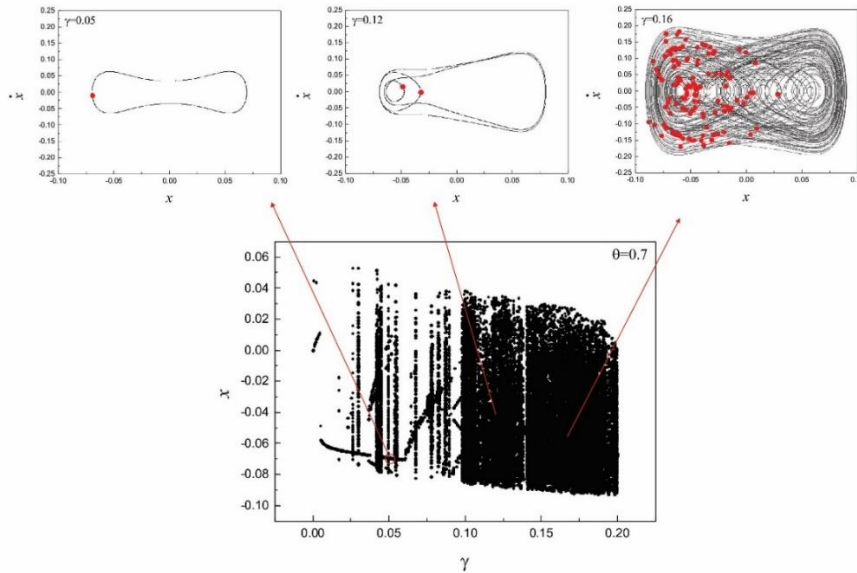


Figure 13: Power considering different values of forcing frequency  $(\theta > \theta_A)$ .

### 5.3 Influence of Forcing Amplitude

Different forcing amplitude conditions are now investigated using  $\bar{\omega} = 1.0$ . Figure 14 and Figure 15 show the bifurcation diagrams of displacement and power for low temperature  $\theta = 0.7$ . The forcing amplitude change causes either transition from periodic response to chaos. By considering high temperature ( $\theta > \theta_A$ ), the system presents a periodic behavior (Fig. 16 and 17). As expected, the system response temperature dependent.



**Figure 14: Dimensionless displacement considering different values of forcing amplitude ( $\theta < \theta_M$ ).**

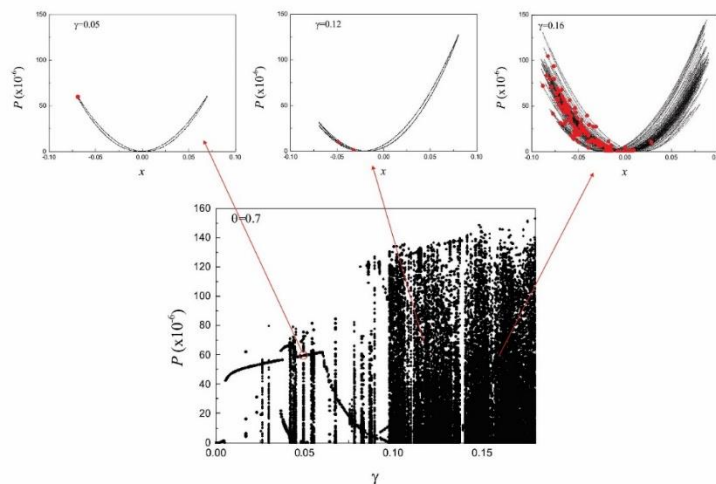


**Figure 15: Power considering different values of forcing amplitude ( $\theta < \theta_M$ ).**

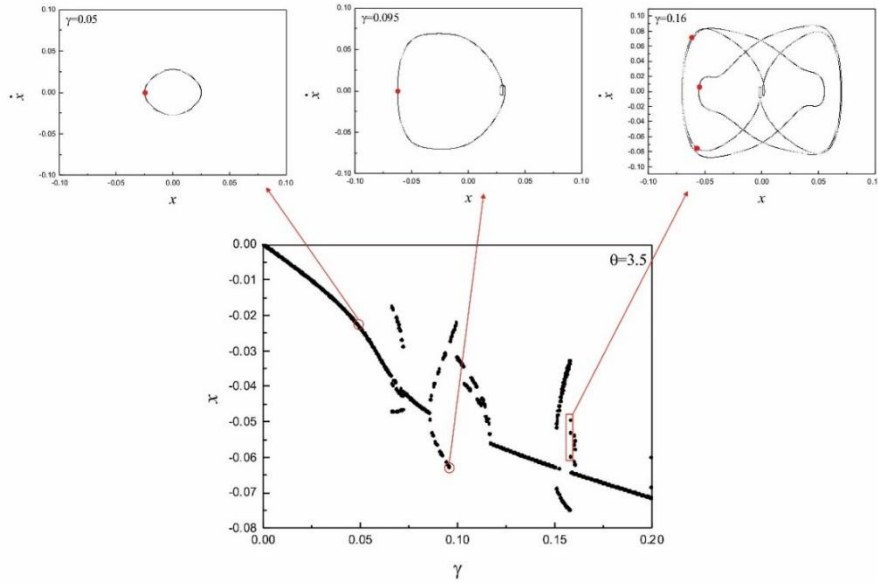


**Figure 16: Dimensionless displacement considering different values of forcing amplitude ( $\theta > \theta_A$ ).**

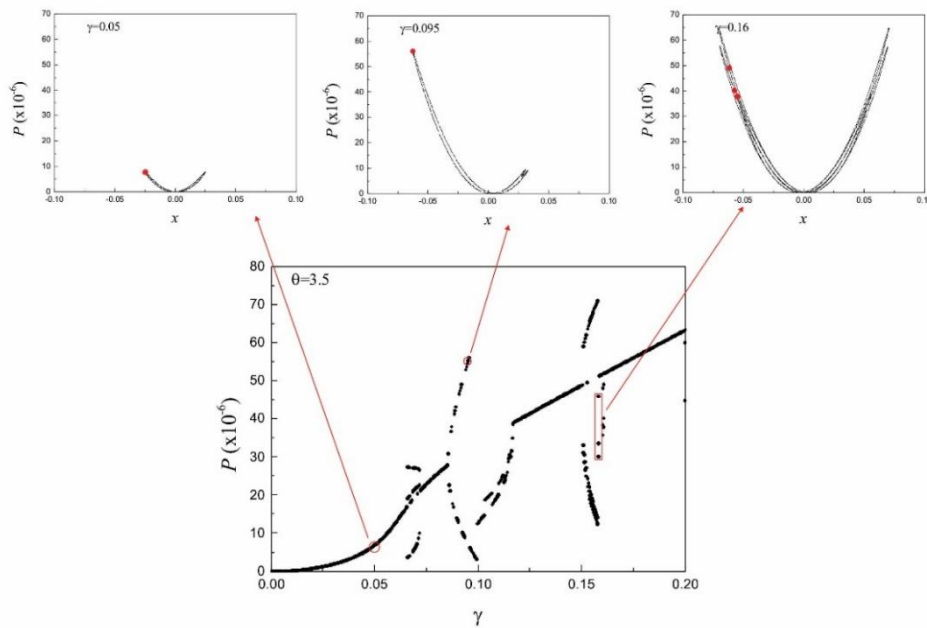


**Figure 17: Dimensionless displacement considering different values of forcing amplitude ( $\theta > \theta_A$ ).**



## 6 CONCLUSIONS

This paper deals with the dynamical response of coupled SMA-piezoelectric energy harvesting system. A polynomial constitutive model is assumed to describe the thermomechanical behavior of the SMA element. Numerical simulations are carried out at different temperatures, forcing frequency and forcing amplitudes showing distinct responses of the system. The analysis of temperature shows how its variation can modify the system response, including periodic and chaotic characteristics. Qualitative results show that chaotic regions can be related to good performance in terms of generated power and therefore, are of special interest in terms of energy harvesting. It is possible to say that the incorporation of the SMA element can be used to extend the operational range of the system, adjusting the system performance in terms of energy harvesting. Nevertheless, it is important to be pointed out that a proper description of the hysteretic behavior of SMA element needs to be carried out in order to confirm some of the conclusions.

## 7 REFERENCES

- Cammarano, A., Neild, S.A., Burrow, S. G., & Inman, D.J., 2014, *The bandwidth of optimized nonlinear vibration-based energy harvesters*, Smart Materials and Structures 23: 055019-055028.
- Du Toit N. E., 2005, *Microelectromechanical systems piezoelectric vibration energy harvester*, Thesis (Ph. D.), Massachusetts Institute of Technology-2006-03-29.
- Erturk, A., Hoffmann, J. & Inman, D.J., 2009, *A piezomagnetoelastic structure for broadband vibration energy harvesting*, Applied Physics Letters 94.25: 254102.
- Erturk, A. & Inman, D.J., 2011a, *Piezoelectric energy harvesting*, John Wiley & Sons.
- Erturk, A. & Inman, D.J., 2011b, *Broadband piezoelectric power generation on high-energy orbits of the bistable Duffing oscillator with electromechanical coupling*, Journal of Sound and Vibration 330.10: 2339-2353.
- Paiva, A. & Savi, M.A., 2006, *An overview of constitutive models for shape memory alloys*, Mathematical Problems in Engineering 2006:56876-56906.
- De Paula, A.S., Inman, D.J. & Savi, M.A., 2015, *Energy harvesting in a nonlinear piezomagnetoelastic beam subjected to random excitation*, Mechanical Systems and Signal Processing 54: 405-416.
- Avirovik, D., Kumar, A., Bodnar R. J. & Priya, S., 2013, *Remote light energy harvesting and actuation using shape memory alloy-piezoelectric hybrid transducer*, Smart Materials and Structures 22: 052001-052007.
- Falk, F., 1980, *Model free-energy, mechanics and thermodynamics of shape memory alloys*, Acta Metallurgica 28:1773-1780.

Silva, L.L., Oliveira, S.A., Pacheco P.M.C.L. & Savi, M.A., 2015, *Synergistic Use of Smart Materials for Vibration-Based Energy Harvesting*, European Physical Journal – Special Topics, 224(14-15): 3005-3012.

Savi, M.A. & Pacheco, P.M.C.L., 2002, *Chaos and hyperchaos in shape memory systems*, *International Journal of Bifurcation and Chaos*, 12(3): 645–657

Ferrari, M., Ferrari, V., Guizzetti, M., Andò, B., Baglio S. & Trigona, C., 2010, *Improved Energy Harvesting from Wideband Vibrations by Nonlinear Piezoelectric Converters*, *Sensors and Actuators A: Physical*, 162:425–431

Rhimi M. & Lajnef, N., 2012, *Modeling of a Composite Piezoelectric/Shape Memory Alloy Cantilevered Beam for Vibration Energy Harvesting*, ASME 2012 Conference on Smart Materials, Adaptive Structures and Intelligent Systems 2: 19-21.

Dutoit N.E. & Wardle, B.L., 2006, *Performance of microfabricated piezoelectric vibration energy harvesters*, *Integrated Ferroelectrics* 83.1: 13-32.

Mitcheson, P.D., Green, T.C., Yeatman, E.M., Holmes & A.S., 2004, *Architectures for vibration-driven micropower generators*, *Journal of Microelectromechanical Systems*, 13:429–440.

Stanton, S.C., Erturk, A., Mann, B.P. & Inman, D.J., 2010, *Nonlinear piezoelectricity in electroelastic energy harvesters: modeling and experimental identification*, *Journal of Applied Physics* 108.7: 074903

Beeby, S.P., Wang, L., Dabin, Z. Weddell, A., Merrett, G.V., Stark, B., Szarka, G. & Al-Hashimi, M.B.M., 2013, *A comparison of power output from linear and non-linear kinetic energy harvesters using real vibration data*, *Smart Materials and Structures*, 22 (7): 075022.

Anton S. R. & Sodano, H.A., 2007, *A review of power harvesting using piezoelectric materials (2003–2006)*, *Smart materials and Structures* 16.3: R1.

Roundy, S., Wright, P.K. & Rabaey, J., 2013, *A study of low level vibrations as a power source for wireless sensor nodes*, *Computer Communications*, 26:1131–1144.

Yang, Y. W., Tang, L.H., & Li, H.Y., 2009, *Vibration energy harvesting using macro-fiber composites*, *Smart Materials and Structures*, 18:115025.